Hydrol. Earth Syst. Sci. Discuss., 10, 5535–5561, 2013
www.hydrol-earth-syst-sci-discuss.net/10/5535/2013/
doi:10.5194/hessd-10-5535-2013

Hydrology and Earth System Sciences
Open Access
Discussions

Using the nonlinear aquifer storage–discharge relationship to simulate the baseflow of glacier and snowmelt dominated basins in Northwest China

R. Gan[1,2] **and Y. Luo**[1]

[1]Key Laboratory of Ecosystem Network Observation and Modeling, Institute of Geographic Sciences and Natural Resources Research, Chinese Academy of Sciences, 100101 Beijing, China
[2]University of Chinese Academy of Sciences, Beijing 100049, China

Received: 20 March 2013 – Accepted: 16 April 2013 – Published: 30 April 2013

Correspondence to: Y. Luo (luoyi.cas@hotmail.com)

Published by Copernicus Publications on behalf of the European Geosciences Union.

Abstract

Baseflow is an important component in hydrological modeling. This process is usually modeled by using the linear aquifer storage–discharge relation approach, although the outflow from groundwater aquifers is nonlinear. To identify the accuracy of baseflow estimates in rivers dominated by snow and/or glacier melt in arid and cold northwestern China, a nonlinear storage–discharge relationship for use in SWAT (Soil Water Assessment Tools) modeling was developed and applied to the Manas River basin in the Tianshan Mountains. Linear reservoir models and a digital filter program were used for comparisons. Meanwhile, numerical analysis of flow recession curves from 78 river gauge stations revealed variation in the coefficients of the nonlinear relationship. It was found that the nonlinear reservoir model can improve the streamflow simulation, especially for low-flows. The highest Nash–Sutcliff efficiency and lowest Percent Bias were obtained when compared to the one- or two-linear reservoir approach. The exponent *b* of the aquifer storage–discharge function varied mostly between 0.0 and 0.1, which is much smaller than the suggested value of 0.5. The coefficient *a* of the function is related to catchment properties, primarily the basin and glacier areas.

1 Introduction

Baseflow is an important component in hydrological modeling. This process is usually modeled by using the linear aquifer storage–discharge relationship approach due to its simplicity (e.g. Nathan and McMahon, 1990; Fenicia et al., 2006; Ferker et al., 2010). Theoretical studies of groundwater flow have shown that a linear storage–discharge relationship describes the groundwater behavior of one-dimensional flow in a confined aquifer, assuming that the thickness and hydraulic conductivity are uniform (Werner and Sundquist, 1951). In this case, the logarithm of the change in discharge varies linearly with time during recession period. However, in most cases, semi-logarithmic plots

HESSD
10, 5535–5561, 2013

of river flow are still concave, which indicates the non-linearity of the aquifer storage–discharge relationship.

The linear aquifer storage–discharge relationship has been proven to be adequate (Chapman, 1999; Fenicia et al., 2006), and the prediction of the model can be improved by combining parallel linear reservoirs if the single linear reservoir fails (Moore, 1997; Luo et al., 2012), Wittenberg (1999) argued that a shallow groundwater aquifer can be divided into independent storage zones, and suggested that a non-linear reservoir function is more realistic than linear models based on the analysis of a variety of streamflow recession curves.

The exponential function $S = a \cdot Q_b^b$ is often adapted to describe the nonlinear aquifer storage–discharge relationship. In this funtion the coefficient a is relevant to the area, porosity, hydraulic conductivity and morphometric properties of the catchment, and the exponent b is related to the properties of the aquifer that can be derived from river streamflow records of the rivers (Wittenberg, 1994, 1999). A value of 0.5 for b appears to be a standard power exponent for an unconfined aquifer (Wittenberg, 1999; Aksoy and Wittenberg, 2011). This may greatly simplify the baseflow simulation. However, values for the exponent b vary significantly among river catchments due to differences in the physical attributes of catchments.

The arid region of northwestern China has an area of 2.66 million square kilometers. More than 95 % of the surface water in this area comes from the 576 rivers originating in the high mountains. Glaciers and snowmelt contribute 30–40 % of the streamflow. Luo et al. (2012) modified the baseflow component of the SWAT (Soil and Water Assessment Tool, Arnold and Fohrer, 2005) model by using two parallel linear reservoirs, achieving a much better streamflow simulation than the original single linear reservoir approach in the Manas River basin in this area.

Thus, the main objectives of this paper are to investigate (1) the performance of the nonlinear aquifer storage–discharge relation using fewer parameters in the baseflow simulation in SWAT and (2) the variability of the coefficients for the rivers in the arid region of northwestern China.

HESSD
10, 5535–5561, 2013

2 Materials and methods

2.1 The nonlinear aquifer storage–discharge function

An exponential function has been used to describe the storage–discharge relationship (Wittenberg, 1999):

$$S = a \cdot Q_b^b \tag{1}$$

where S is the aquifer storage in m^3, Q_b is the discharge rate in $m^3 s^{-1}$ and the factor a has the dimension of $m^{3-3b} s^b$. If volumes are expressed as heights over a unit area and the time interval is a day, then the units of a are in $mm^{1-b} d^b$ and the exponent b is dimensionless. The linear reservoir is thus a special case with $b = 1$. Outflow from the aquifer can be derived using Eq. (1),

$$Q_b = (S/a)^{\frac{1}{b}} \tag{2}$$

The constants a and b can be derived from the observed flow recession curves. Based on Eq. (1) and the continuity equation of the aquifer storage,

$$dS/dt = -Q \tag{3}$$

Wittenberg (1999) derived the discharge rate of the aquifer at time t:

$$Q_t = Q_0 \left[1 + \frac{(1-b)Q_0^{1-b}}{ab} t \right]^{\frac{1}{b-1}} \tag{4}$$

where Q_t is the discharge rate at time t, and Q_0 is the discharge rate at the beginning of interest.

The nonlinear aquifer storage–discharge function expressed by Eq. (2) is embedded into the SWAT model to simulate the baseflow process. The performance of the

HESSD
10, 5535–5561, 2013

nonlinear approach, the one-reservoir linear approach originally provided by the SWAT model (Neistch et al., 2002), the two-reservoir approach by Luo et al. (2012), and the automatic digital filter technique (Nathan and McMahon, 1990) can be then compared.

2.2 SWAT model setup and parameterization

The Manas River basin (MRB) is described in detailed by Luo et al. (2012). This study used the SWAT model setup and parameters by Luo et al. (2012), and the constants in Eq. (2) have been optimized. In the Manas River basin, the daily streamflow records at the Kenswat Hydrological Station (KHS) from 1961 to 1999 indicate that low-flow occurs during October to March, which has been confirmed by Luo et al. (2012). The influence of groundwater evaporation on the recession can be neglected. Therefore, the low-flow period from October to March was selected as the period used to fit the recession curve. The parameters *a* and *b* can be optimized by fitting the calculated discharge curves to the observed recession curves. The parameters *a* and *b* for the MRB were used in the SWAT model to simulate the baseflow processes. The performance of the nonlinear baseflow approach was evaluated using the Nash–Sutcliff Efficiency (NSE), the Percent Bias (PBIAS) and their ranking system (Morasi et al., 2007). The parameters *a* and *b* were also analyzed for other 78 basins in this region to investigate their variability among different basins and their relationships to the catchment attributes.

3 Results and discussion

3.1 Aquifer storage–discharge relationship for the MRB

The aquifer discharge does not show a linear change over time on the semi-log plot (Fig. 1). This may be due to complicated factors, such as climate, topography, land cover such as snow and glaciers, soil types and catchment geology (Haberlandt et al., 2001; Mwakalila et al., 2002; Longobardi and Villani, 2008).

HESSD
10, 5535–5561, 2013

The optimized values for *a* and *b* are listed in Table 1, and the discharge curves calculated using Eq. (4) with these values are presented in Fig. 1. Surprisingly, the value of *b* is far less than the suggested value, which is approximately 0.5 (Wittenberg, 1994, 1999). Due to an exponent as small as 0.025, the aquifer discharge rate appears to be strongly related to the aquifer storage. The recession data calculated using Eq. (4) was compared to the observed data and those calculated using the linear relation. Compared to the observed low flow, the linear relation underestimates the discharge in the low range and overestimates it in the mid and upper-range (Fig. 2a), while the nonlinear relation estimates the discharge well for the low and mid ranges and slightly underestimates it in the upper range (Fig. 2b). Generally, the nonlinear relation performs much better than the linear relation.

3.2 The simulated streamflow

The performances of the different baseflow simulation approaches are presented in Table 2. The NSE and PBIAS indicate that the one-nonlinear reservoir method and the two-linear reservoir method both yield "good" or "very good" results based on the rating rules given by Moriasi et al. (2007), which are better than the original one-linear reservoir method. The NSEs of the one-nonlinear reservoir approach are relatively similar compared with the two-linear reservoir approach. The PBIASs of the one-nonlinear reservoir method seem slightly better than those of the two-linear reservoir approach.

The Streamflow processes simulated by the SWAT model using different baseflow approaches were compared to the measured values. A six-year period of data at validation stage was taken to give as an example (Fig. 3). In general, the simulated streamflow processes show a similar trend to those observed for the different models. The flow starts to rise in late April due to snowmelt. The glacier begins to melt when the snowpack depletes, and the streamflow continues to rise until the peak discharge in late July, then the streamflow recedes until the glacier ceases to melt in late September, after which the streamflow remains relatively stable recession until the next April. It is a common feature for rivers dominated by snow/glacier melt in northwestern China.

HESSD
10, 5535–5561, 2013

During the low-flow period (from November to April), the one-linear reservoir model underestimates the streamflow significantly (Fig. 3a), while the one-nonlinear reservoir model and two-linear reservoir model simulation improve the simulation remarkably (Fig. 3b). However, most of the discrepancies occur during the high-discharge periods, when frequent precipitation and snow/glacier melt occurred. This may be attributed to the snowmelt simulation (Arnold et al., 2000). Luo et al. (2012) also found significant differences between the simulated and measured maximum flow volumes, and thought that these differences might be due to uncertainty in the meteorological input in mountainous areas, which are derived from records taken at the foot of the mountain using a single precipitation lapse rate.

Slight differences between the simulated and measured annual flow volumes exist for the two-linear reservoir and one-nonlinear baseflow simulation approaches. The nonlinear approach overestimates the annual flow volume by 1.1 %, and the two-linear reservoir approach overestimates it by 3.1 %. Both can be ranked as "very good" according to the ranking system of Morasi et al. (2007).

3.3 The simulated baseflow

The observed streamflow eventually became nearly constant, which is sustained by outflow from groundwater. The simulated baseflow and surface flow hydrographs using one-nonlinear reservoir model are shown in Fig. 4. The streamflow is dominated by baseflow during the low-flow period, while surface flow is larger than baseflow in the high-flow period, when rainfall and snow/glacier melting occur.

The surface flow responds closely to the recharge caused by rainfall events and snow/glacier melting. The pattern of surface flow during the high-flow period obtained from the SWAT model demonstrates a fast and transient response in recharge; the surface flow fluctuates. However, the baseflow response during the high-flow period does not follow the same surface flow response: its response is smooth (Fig. 4). Partington et al. (2012) found that an abrupt change in baseflow occurs at the beginnings and ends of the rainfall events when using the HGS model. This may be because the

HESSD
10, 5535–5561, 2013

catchment is small, the infiltration capacity of the sand is high, and the vertical extent of the unsaturated zone is less than 1 m, resulting in a rapid response in the baseflow. McCuen (2005) found a smooth and delayed response for baseflow hydrographs, rather than an abrupt change. During the low-flow period, both the baseflow and surface flow processes are relatively stable.

The average monthly flow processes from 1966 to 1999 using a one-nonlinear reservoir model and filter method are shown in Fig. 5. The model-based baseflow begins to rise in May, peaks in August, and quickly returns to the sluggish receding stage. It indicates a groundwater recharge of rainfall and snow/glacier melt water during the summer, which then releases slowly during the winter and spring. The aquifer storage fluctuates seasonally in the simulation. Interestingly, the onset of the rising limb in the one-nonlinear model-based surface flow hydrograph differs from that of the baseflow, which matches the streamflow hydrograph well. The simulated surface flow startes to rise in April, and reaches its peak in July, both earlier than the simulated baseflow. The Manas River basin is dominated by snow/glacier meltwater, and the snowmelt usually starts in the middle of April. The surface flow responds to snowmelt immediately, while the infiltration and recharge increase the time to groundwater discharge, resulting in a delay in the baseflow component of streamflow.

The time delays to the onset of baseflow based the one-nonlinear model and linear reservoir model are much longer than the time delays to the increase in filter-based baseflow (Figs. 5, 6). During this period, the soil in the Manas River basin is frozen. Luo et al. (2012) proposed that the infiltration and recharge from the soil profile during freezing and thawing eventually determines the onset of the rising limb. However, the freezing and thawing processes of soil have been insufficiently described in most watershed hydrological models, and this needs more detailed description. Partington et al. (2012) found that separation methods might miss the dynamics of baseflow. The peak times, the model- and filter-based baseflow are similar, except for the one-linear reservoir model, which reaches the peak earlier.

HESSD
10, 5535–5561, 2013

Figure 6 illustrates the baseflow hydrographs obtained using different modeling and filter methods. There is a good agreement in the baseflow patterns of the SWAT and filter methods. All of the approaches capture the change in slope of the recession in late September, when the direct surface runoff usually ceases recharging the groundwater storage. The magnitude of the baseflow differs among the four estimation methods. The one-linear reservoir model significantly underestimates the baseflow during the low-flow period compared to the filter-based baseflow, which might be the cause of the underestimated streamflow. The two-linear and one-nonlinear reservoir models reproduce the baseflow properly during the low-flow period. During the high-flow period, the model-based baseflow is smaller than the filter-based baseflow.

The average annual baseflow volumes and baseflow index (BFI) calculated as the long-term ratio of the baseflow volume to the total streamflow volume, according to the definition of the Institute of Hydrology (1980), are listed in Table 3. The average annual baseflow volume determined using the digital filter separation method is 7.2×10^8 m^3, and the simulated values using the one-linear, two-linear and one-nonlinear reservoir models are 5.63×10^8 m^3, 5.62×10^8 m^3, and 5.38×10^8 m^3 respectively. The one-linear and two-linear reservoir models give similar annual baseflow volumes that are slightly larger than that from the one-nonlinear reservoir model. The digital filter method gives a much larger baseflow volume than the model-based approaches.

The baseflow index for the one-linear, two-linear and one-nonlinear reservoir models are 0.45, 0.45, and 0.44 respectively, and the filter-based index is 0.60. The model estimates in this study are 22 to 25 % lower than that of the digital filter method. Wu et al. (2007) found that the SWAT estimate is lower than that of the Rutledge method, and attributed it primarily to the long time lag between the winter snowpack accumulation and the spring snow melting events. In this period, the Rutledge method includes baseflow due to its assumptions about the temporal offset between precipitation events and the runoff response, while the SWAT model method more correctly treats this as surface runoff. Snowmelt is an important component of streamflow in the Manas River basin, which may be the reason for the underestimation of the SWAT method in this

HESSD
10, 5535–5561, 2013

study. Additionally, the streamflow in the SWAT model comprises surface runoff, lateral subsurface flow, and baseflow, while in the digital filter method, streamflow consists of surface runoff and baseflow. Thus the digital filter method may treat the lateral subsurface flow in the SWAT method as baseflow. The average annual lateral flow volume is 1.78×10^8 m^3, and the sum of the baseflow volume and the lateral flow volume in the one-nonlinear reservoir model is 7.16×10^8 m^3, accounting for 58 % of the average annual streamflow, which is similar to the baseflow index given by the filter-based. The one-linear and two-linear reservoir models provide similar results. It is difficult to determine which is more representative due to the challenges in measuring baseflow in the field.

3.4 The groundwater storage

The averaged monthly groundwater storage calculated by the SWAT model using the nonlinear approach for MRB is shown in Fig. 7. The maximum, minimum, and mean storage water depths are 782.1, 702.1, and 737.5 mm, respectively. There is seasonal variation in the groundwater storage. It begins to rise in May, reaches its peak in August, starts to decrease in September, and reaches its lowest value in April. The seasonal pattern of storage water depth is related to the possible times for recharge. The sudden rise in storage volume in the month of May could be the result of recharge by snowmelt. It continues to increase due to additional snow/glacier melting. In July, the maximum recharge occurs due to greater glacier melting and rainfall. Then the rainfall and glacier meltwater starts to decrease, as does the recharge. In September, the recharge is lower than the discharge, and the storage water depth begins to decline. From October to the following April, the recharge ceases, but the groundwater discharge continues, which is the main contribution to streamflow during this period, and the storage water depth continues to decrease.

HESSD
10, 5535–5561, 2013

3.5 Variation in the parameters *a* and *b*

To investigate the variability in the coefficient *a* and the exponent *b* in the exponential aquifer storage–discharge function among different catchments, *a* and *b* were optimized for 78 catchments in this region with different physical features, such as drainage area, and glacier cover ratio, using the observed daily flow records.

The statistics indicate that the exponent *b* varies significantly among catchments (Table 4). For the investigated catchments, the mean value for the exponent *b* is 0.32. Wittenberg (1994) found that the exponent *b* ranges from 0.11 to 0.91, with a typical value of 0.4 for 17 gauging stations in northwestern Germany, and Chapman (1999) found that it varies between 0.31 and 0.63 for 11 catchments in eastern Australia. The analysis of observed flow recession in numerous rivers in different hydrological regimes (Wittenberg, 1994, 1999) yielded values of $b < 1$, peaking between 0.3 and 0.4, with a mean value of $b \approx 0.5$. In our study, the exponent b varies more widely, from 0.02 to 1.0 (Table 4), with a skewed distribution. The smaller exponent indicates that the aquifer discharge is more sensitive to changes in the aquifer storage, based on Eq. (1). When *b* equals 1.0, the equation implies that the discharge changes linearly with the storage. The exponent *b* reflects the influences of the aquifer properties upon the discharge. Harman and Sivapalan (2009) indicated that *b* was never below 0.5 in the homogeneous, planar hill slopes. Chapman (1999) suggested that smaller exponents may be attributed to the horizontal and vertical convergence of the flow in source areas, and the value of 0.5 for *b* appears to be a standard power exponent for unconfined aquifers (Wittenberg, 1999; Aksoy et al., 2012). These might imply that aquifer properties are more varied in this region, and the exponent *b* should be specific for a catchment, not simply the mean value of 0.32 or the suggested value of 0.5. Nevertheless, the coefficients of determination (R^2) of the catchments indicate that for most catchments, the nonlinear exponential function describes the recession processes very well.

The parameter *a* is related to some of the catchment attributes. Regression analysis indicates that *a* is significantly correlated to the catchment area and the glacier area

HESSD
10, 5535–5561, 2013

within the catchment (Table 5). The parameter *a* may vary seasonally, which may be attributed to the variation in the hydraulic gradient caused by the changes in evapotranspiration losses (Aksoy and Wittenberg, 2011; Datta et al., 2012).

4 Conclusions

This study indicates that the nonlinear aquifer storage–discharge approach performs as well as the two-linear reservoir approach in the Manas River basin, Xinjiang, China, and has the advantage of a simpler form and only two parameters that must be calibrated. The parameters *a* and *b* in the exponential function that describe the aquifer storage–discharge relationship can be calibrated independently from the observed streamflow data.

The parameters *a* and *b* vary significantly among the rivers in the arid region of northwestern China. The constant *b* ranges from 0.015 to 1, with a mean value of 0.32 and a standard deviation of 0.35. Of the 78 basins investigated, almost half of their b values fall between 0 and 0.1. Overall, the exponential aquifer storage–discharge function fits the recession processes very well for most of the catchments.

Acknowledgements. This study is supported partially by the 973 Program of China (Grant No. 2010CB951002), the Natural Science Foundation of China (Grant No. 41130641), and the Project of the National Eleventh-Five Year Research Program of China (Grant No. 2012BAC19B07).

References

Aksoy, H. and Wittenberg, H.: Nonlinear baseflow recession analysis in watersheds with intermittent streamflow, Hydrolog. Sci. J., 56, 226–237, 2011.

Arnold, J. and Fohrer, N.: SWAT2000: current capabilities and research opportunities in applied watershed modeling, Hydrol. Process., 19, 563–572, 2005.

HESSD

10, 5535–5561, 2013

Arnold, J. G., Muttiah, R. S., Srinivasan, R., and Allen, P. M.: Regional estimation of base flow and groundwater recharge in the Upper Mississippi River basin, J. Hydrol., 227, 21–40, 2000.
Chapman, T.: A comparison of algorithms for stream flow recession and baseflow separation, Hydrol. Process., 13, 701–714, 1999.
Chu, T. W. and Shirmohammadi, A.: Evaluation of the SWAT model's hydrology component in the Piedmont physiographic region of Maryland, T. ASAE, 47, 1057–1073, 2004.
Datta, A. R., Bolisetti, T., and Balachandar, R.: Automated linear and nonlinear reservoir approaches for estimating annual baseflow, J. Hydrol. Eng., 17, 554–564, 2012.
Eckhardt, K.: A comparison of baseflow indices, which were calculated with seven different baseflow separation methods, J. Hydrol., 352, 168–173, 2008.
Essery, C. I.: Influence of season and balance period on the construction of catchment water balances, J. Hydrol., 130, 171–187, 1992.
Fenicia, F., Savenije, H. H. G., Matgen, P., and Pfister, L.: Is the groundwater reservoir linear? Learning from data in hydrological modelling, Hydrol. Earth Syst. Sci., 10, 139–150, doi:10.5194/hess-10-139-2006, 2006.
Ferket, B. V. A., Samain, B., and Pauwels, V. R. N.: Internal validation of conceptual rainfall-runoff models using baseflow separation, J. Hydrol., 381, 158–173, 2010.
Haberlandt, U., Klocking, B., Krysanova, V., and Becker, A.: Regionalisation of the base flow index from dynamically simulated flow components – a case study in the Elbe River Basin, J. Hydrol., 248, 35–53, 2001.
Harman, C. J. and Sivapalan, M.: A similarity framework to assess controls on shallow subsurface flow dynamics in hillslopes, Water Resour. Res., 45, W01417, doi:10.1029/2008WR007067, 2009.
Kirchner, J. W.: Catchments as simple dynamical systems: catchment characterization, rainfall–runoff modeling, and doing hydrology backward, Water Resour. Res., 45, W02429, doi:10.1029/2008WR006912, 2009.
Longobardi, A. and Paolo, V.: Baseflow index regionalization analysis in a mediterranean area and data scarcity context: role of the catchment permeability index, J. Hydrol., 355, 63–75, 2008.
Luo, Y., Arnold, J., Allen, P., and Chen, X.: Baseflow simulation using SWAT model in an inland river basin in Tianshan Mountains, Northwest China, Hydrol. Earth Syst. Sci., 16, 1259–1267, doi:10.5194/hess-16-1259-2012, 2012.

HESSD
10, 5535–5561, 2013

McCuen, R. H.: Hydrologic Analysis and Design, Prentice Hall, 2005.
Moore, R. D.: Storage-outflow modelling of streamflow recessions, with application to a shallow-soil forested catchment, J. Hydrol., 198, 260–270, 1997.
Moriasi, D. N., Arnold, J., Van Liew, M. W., Bingner, R. L., Harmel, R. D., and Veith, T. L.: Model evaluation guidelines for systematic quantification of accuracy in watershed simulations, T. ASABE, 50, 885–900, 2007.
Mwakalila, S., Feyen, J., and Wyseure, G.: The influence of physical catchment properties on baseflow in semi-arid environments, J. Arid Environ., 52, 245–258, 2002.
Nathan, R. J. and McMahon, T. A.: Evaluation of automated techniques for baseflow and recession analysis, Water Resour. Res., 26, 1465–1473, 1990.
Neitsch, S. L., Arnold, J. G., Kiniry, J. R., Williams, J. R., and King, K. W.: Soil water assessment tool theoretical document, version 2000, Grassland, Soil and Water Research Laboratory, Temple, Texas, 506 pp., 2002.
Partington, D., Brunner, P., Simmons, C. T., Therrien, R., Werner, A. D., Therrien, R., Maier, H. R., and Dandy, G. C.: Evaluation of outputs from automated baseflow separation methods against simulated baseflow from a physically based, surface water-groundwater flow model, J. Hydrol., 458–459, 28–39, 2012.
Peterson, J. R. and Hamlet, J. M.: Hydrologic calibration of the SWAT model in a watershed containing fragipan soils, J. Am. Water Resour. As., 34, 531–544, 1998.
Rupp, D. E. and Woods, R. A.: Increased flexibility in base flow modelling using a power law transmissivity profile, Hydrol. Process., 22, 2667–2671, 2008.
Samuel, J., Coulibaly, P., and Metcalfe, R. A.: Identification of rainfall-runoff model for improved baseflow estimation in ungauged basins, Hydrol. Process., 26, 356–366, 2012.
Szilagyi, J., Gribovski, Z., and Kalicz, P.: Estimation of catchment-scale evapotranspiration from baseflow recession data: numerical model and practical application results, J. Hydrol., 336, 206–217, 2007.
Werner, P. W. and Sundquist, K. J.: On the groundwater recession curve for large watersheds, in IASH General Assembly, Brussels, IAHS-AISH P., 33, 202–212, 1951.
Wittenberg, H.: Nonlinear analysis of flow recession curves, in: FRIEND: Flow Regimes from International Experimental and Network Data (Proceeding of the Braunschweig conference, October 1993), IAHS Publ. no. 221. 61–67, 1994.
Wittenberg, H.: Baseflow recession and recharge as nonlinear storage processes, Hydrol. Process., 13, 715–726, 1999.

HESSD
10, 5535–5561, 2013

Wittenberg, H. and Sivapalan, M.: Watershed groundwater balance estimation using streamflow recession analysis and baseflow separation, J. Hydrol., 219, 20–33, 1999.
Wu, K. and Johnston, C. A.: Hydrologic response to climatic variability in a Great Lakes Watershed: a case study with the SWAT model, J. Hydrol., 337, 187–199, 2007.

HESSD
10, 5535–5561, 2013

Table 1. Parameter values of the exponential aquifer storage – discharge function for the Manas River basin, Xinjiang, China.

Approach	Parameter	Calibrated value	R^2
Nonlinear storage–discharge function	*a*	771.6	0.90
	b	0.025	

HESSD
10, 5535–5561, 2013

Table 2. The NSE and PBIAS for the simulated discharge by SWAT model using the different baseflow approaches in the Manas River basin, Tianshan, China.

Model	Segment	NSE	Rating*	PBIAS	Rating*
One-linear reservoir	calibration	0.68	Good	−4.0	Very good
	validation	0.62	Satisfactory	−3.5	
	overall	0.65	Good	−3.7	
Two-linear reservoir	calibration	0.76	Very good	−2.6	Very good
	validation	0.69	Good	−3.6	
	overall	0.72	Good	−3.2	
One-nonlinear reservoir	calibration	0.74	Good	1.8	Very good
	validation	0.70	Good	−3.2	
	overall	0.72	Good	−1.1	

* The rating is based on rules given by Moriasi et al. (2007).

HESSD
10, 5535–5561, 2013

Table 3. Statistical analysis for the baseflow volume and index.

	Filter	One-linear reservoir	Two-linear reservoir	One-nonlinear reservoir
Baseflow volume (10^8 m^3)	7.20	5.63	5.62	5.38
Baseflow index	0.60	0.45	0.45	0.44

HESSD
10, 5535–5561, 2013

Table 4. Statistical analysis for the exponent b of the aquifer storage–discharge function.

b		b				R^2		
	catchments	max	min	mean	stdev	max	min	mean
0.0–0.1	38	0.09	0.02	0.04	0.02	0.90	0.27	0.65
0.1–0.2	8	0.19	0.11	0.15	0.03	0.88	0.36	0.74
0.2–0.3	1	0.25	0.25	0.25	–	0.63	0.63	0.63
0.3–0.4	3	0.40	0.37	0.39	0.02	0.81	0.61	0.68
0.4–0.5	4	0.48	0.43	0.47	0.03	0.88	0.88	0.88
0.5–0.6	2	0.54	0.53	0.54	0.01	0.75	0.36	0.55
0.6–0.7	4	0.69	0.61	0.67	0.04	0.84	0.82	0.83
0.7–0.8	5	0.80	0.72	0.77	0.03	0.84	0.77	0.80
0.8–0.9	3	0.86	0.82	0.84	0.02	0.80	0.70	0.75
0.9–1.0	9	1.00	0.95	0.99	0.02	0.92	0.75	0.83
0.0–1.0	78	1.00	0.02	0.32	0.35	0.92	0.27	0.71

HESSD
10, 5535–5561, 2013

Table 5. Correlation matrix for the parameter and the basin features.

	a	Catchment area	Glacier area
a	1		
Catchment area	0.36[2]	1	
Glacier area	0.26[1]	0.73[2]	1

[1] Correlation is significant at the 0.05 level (2-tailed).
[2] Correlation is significant at the 0.01 level (2-tailed).

HESSD
10, 5535–5561, 2013

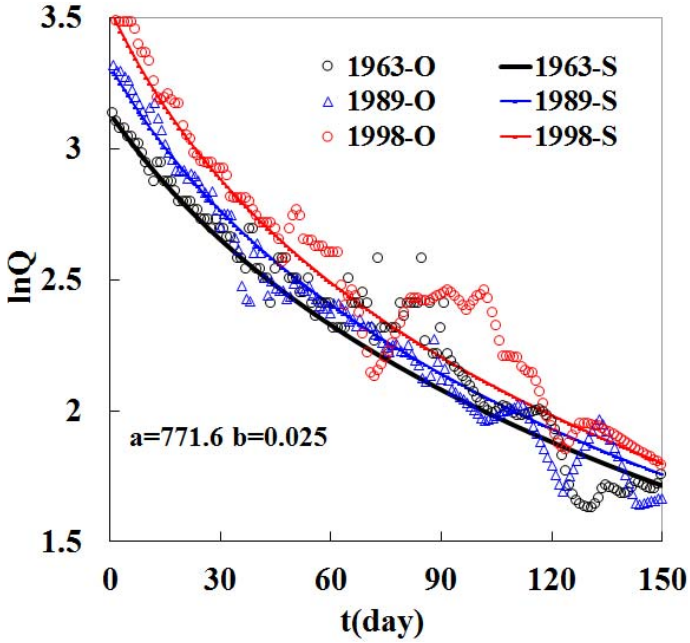

Fig. 1. Recession curves of $\ln Q - t$ of baseflow for typical years in the Manas River basin (O–observed flow; S–simulated flow).

HESSD
10, 5535–5561, 2013

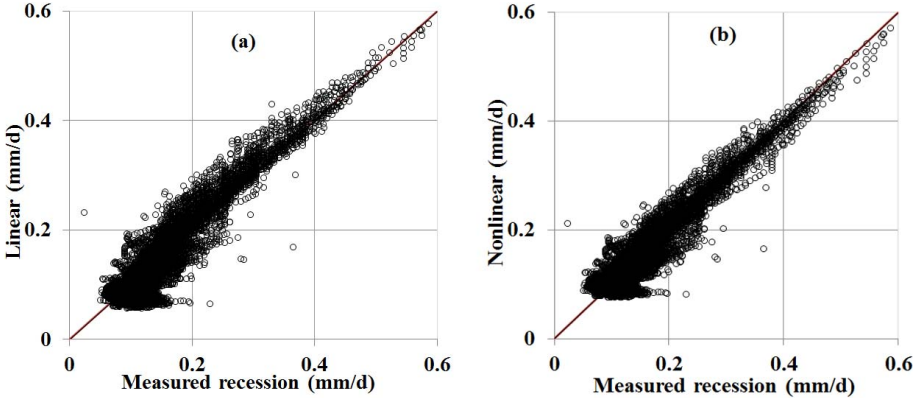

Fig. 2. Comparison of the fitted and measured recession data for 1961–1999 in the Manas River basin. **(a)** Using the linear aquifer storage–discharge relation; **(b)** using the nonlinear aquifer storage–discharge relation.

HESSD
10, 5535–5561, 2013

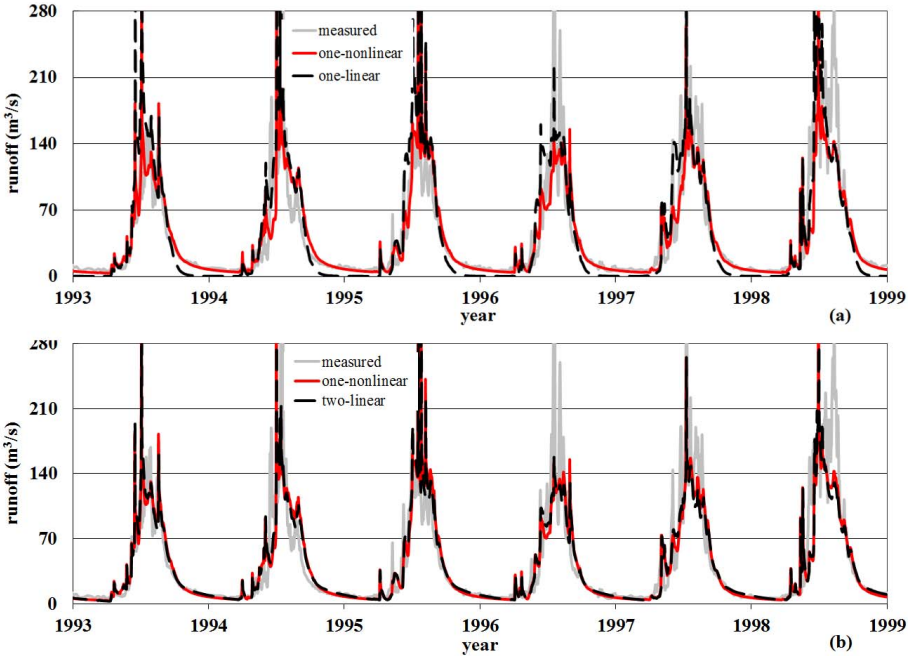

Fig. 3. Comparison of simulated and measured streamflow processes for the validation stage.

HESSD
10, 5535–5561, 2013

The nonlinear aquifer storage–discharge relationship

R. Gan and Y. Luo

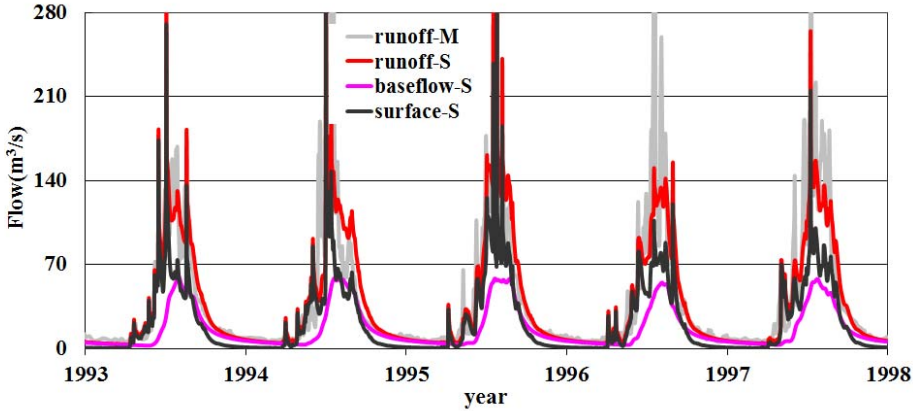

Fig. 4. The simulated baseflow and surface flow processes for the validation stage (M = measured; S = simulated).

HESSD
10, 5535–5561, 2013

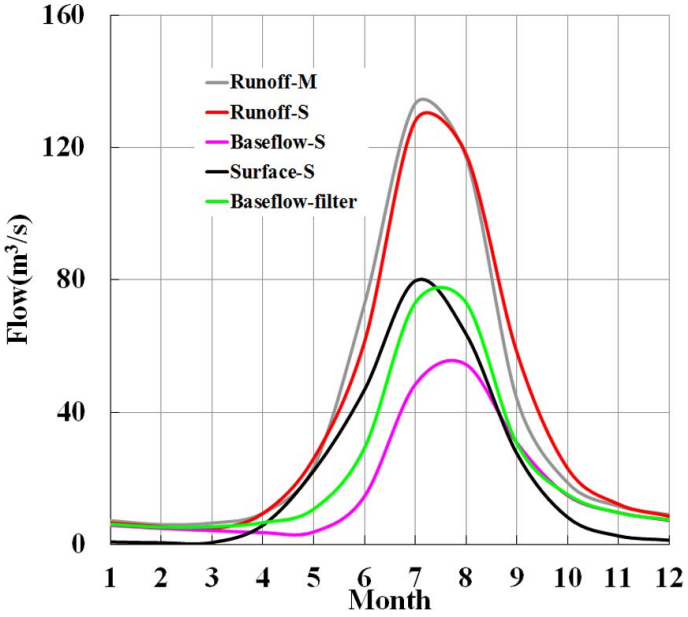

Fig. 5. A comparison of the average monthly baseflow and surface flow processes (M = measured; S = simulated).

HESSD
10, 5535–5561, 2013

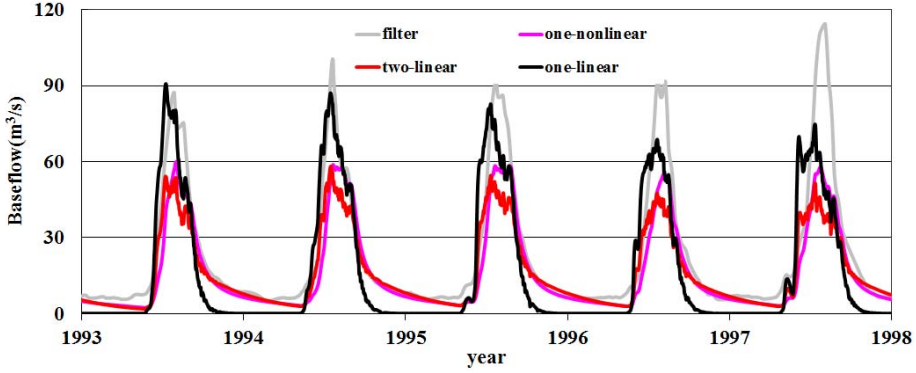

Fig. 6. The baseflow processes generated using the model- and filter-based approaches.

HESSD
10, 5535–5561, 2013

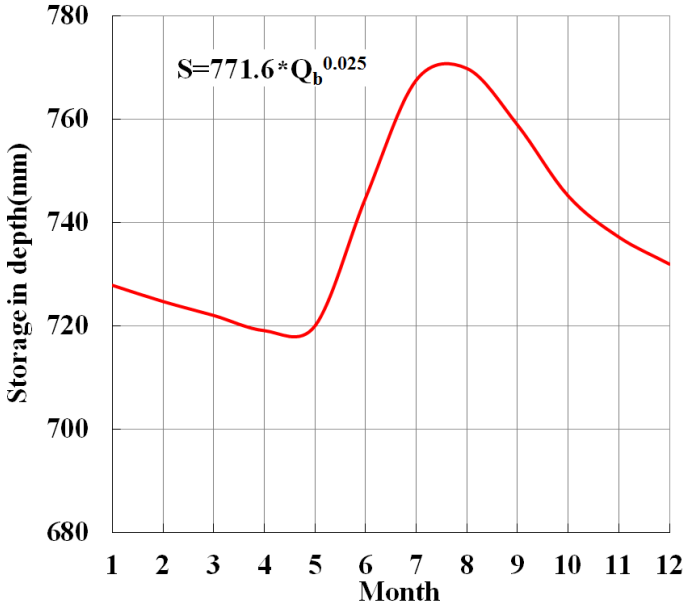

Fig. 7. The storage depth calculated using the nonlinear model approach.

HESSD
10, 5535–5561, 2013